Structure-Based Design of Substituted Diphenyl Sulfones and Sulfoxides as Lipophilic Inhibitors of Thymidylate Synthase

Terence R. Jones,*,† Stephen E. Webber, Michael D. Varney, M. Rami Reddy,‡ Kathleen K. Lewis, Vinit Kathardekar, Hormoz Mazdiyasni, Judith Deal, Dzuy Nguyen, Katharine M. Welsh, Stephanie Webber, Amanda Johnston, David A. Matthews, Ward W. Smith, Cheryl A. Janson, Russell J. Bacquet,§ Eleanor F. Howland, Carol L. J. Booth, Steven M. Herrmann, Robert W. Ward, Jennifer White, Charlotte A. Bartlett, and Cathy A. Morse

Agouron Pharmaceuticals, Inc., 3565 General Atomics Court, San Diego, California 92121

Received August 26, 1996⊗

Six new diphenyl sulfoxide and five new diphenyl sulfones were designed, synthesized, and tested for their inhibition of human and *Escherichia coli* thymidylate synthase (TS) and of the growth of cells in tissue culture. The best sulfoxide inhibitor of human TS was 3-chloro-*N*-((3,4-dihydro-2-methyl-4-oxo-6-quinazolinyl)methyl)-4-(phenylsulfinyl)-*N*-(prop-2-ynyl)-aniline (**7c**) that had a K_i of 27 nM. No sulfone improved on TS inhibition by the previously reported 4-(*N*-((3,4-dihydro-2-methyl-6-quinazolinyl)methyl)-*N*-prop-2-ynylamino)phenyl phenyl sulfone (K_i = 12 nM). Nevertheless, one sulfone, 4-((2-chlorophenyl)sulfonyl)-*N*-((3,4-dihydro-2-methyl-4-oxo-6-quinazolinyl)methyl)-*N*-(prop-2-ynyl)aniline, was selected, on the basis of its inhibition of both TS and cell growth, for antitumor testing; it gave a 61% increase in life span to mice bearing the thymidine kinase-deficient L5178Y (TK^-) lymphoma. A crystal structure of *N*-((3,4-dihydro-2-methyl-4-oxo-6-quinazolinyl)methyl)-4-((2-methylphenyl)sulfinyl)-*N*-(prop-2-ynyl)aniline complexed with *E. coli* TS was solved and revealed selective binding of one sulfoxide enantiomer. AMBER calculations showed that the enantioselection was due to asymmetric electrostatic effects at the mouth of the active site. In contrast, a similar crystal structure of the sulfoxide **7c**, along with AMBER calculations, indicated that both enantiomers bound, but with different affinities. The side chain of Phe176 shifted in order to structurally accommodate the chlorine of the more weakly bound enantiomer.

The first papers in this series[1,2] described the development of the quinazoline-based diphenyl sulfone **8a** (Scheme 1) as a 12 nM lipophilic inhibitor of the enzyme thymidylate synthase. This enzyme is crucially involved in DNA synthesis, and inhibitors of it have potential as cytotoxic therapeutics. Because some simple meta-substituted propargylanilines had enhanced the inhibition of thymidylate synthase (TS), we synthesized and tested a meta-substituted analogue of **8a** (**8d**, Table 1), but it inhibited TS no better than **8a**.[1,2] In this paper we further explore structure−activity relationships in the diphenyl sulfone series and describe new substituted sulfones and also, given the flexibility of the synthetic route used, the corresponding series of diphenyl sulfoxides.

Design of Inhibitors

The report[1,2] of the X-ray crystal structure of the trifluoromethyl-substituted compound **8d** bound to *Escherichia coli* TS revealed that, relative to the unsubstituted parent compound, the entire diphenyl sulfone moiety had moved upward toward residues Phe176 and His51, a movement that might possibly explain the unimproved inhibition observed for **8d**. It seemed possible that the CF_3 substituent might not be fitting properly into the so-called meta pocket[1,2] and that smaller substituents X might show some advantage. Therefore the fluoro and chloro compounds **8b** and **8c**, respectively, were modeled and minimized by AM1, and their low-energy structures were docked and compared with the X-ray-derived structure of **8a** in the mouth of the enzyme active site. Both compounds fitted well with the substituents, neatly filling the meta pocket. Earlier consideration had been given to substituents rooting from the distal phenyl ring. From a close examination of the three-dimensional structure of *E. coli* TS[3] (with 10-propargyl-5,8-dideazafolic acid removed and with **8a** modeled in its place since this was before the ternary complex of **8a** had actually been solved) specifically in the region where the SO_2 group linked the distal phenyl ring, there was seen an unoccupied pocket created by the ring of Phe176, the side chain of Ile79, and the methylene of His51. This small region could be accessed from the ortho position of the distal phenyl ring of **8a**, and it was found that either a methyl group or a chlorine had the optimum steric and hydrophobic requirements for van der Waals interactions. AM1 minimization calculations were performed on compounds **8e** and **8f**, and their low-energy structures were docked into the enzyme active site and compared with the model of the parent diphenyl sulfone **8a**. Only slight differences were observed between the two sets of $C-SO_2-C$ torsion angles. It should be noted that in each case these ortho substituents could adopt an alternate configuration with respect to the enzyme. A rotation of 180° about the SO_2−distal phenyl bond would place the methyl or chlorine toward the side chain of Ala262. The disubstituted compound **8g** with inner CF_3 and outer CH_3 substituents had been successfully modeled by AM1 as

* To whom correspondence should be addressed.
† Present address: Ångstrom Pharmaceuticals, Inc., 11772 Sorrento Valley Rd., #101, San Diego, CA 92121.
‡ Present address: Gensia, Inc., 9360 Towne Center Drive, San Diego, CA 92121.
§ Deceased.
⊗ Abstract published in *Advance ACS Abstracts,* February 1, 1997.

S0022-2623(96)00613-9 CCC: $14.00

Scheme 1

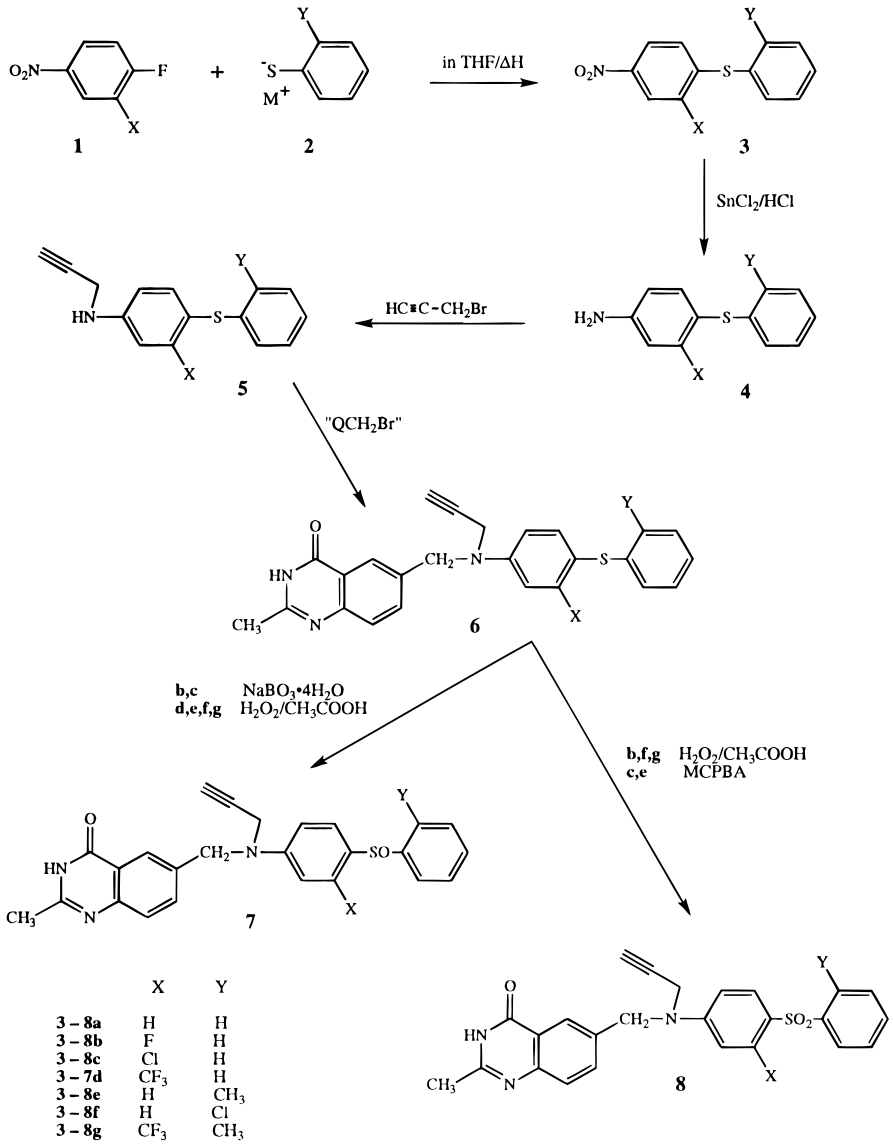

above and selected for synthesis but before the detrimental effect of the CF_3 group in the monosubstituted compound **8d** became fully apparent from the X-ray crystal structure.[1]

Chemistry

Six diphenyl sulfoxides, **7b**−**g**, and five diphenyl sulfones **8b**,**c**,**e**−**g**, were synthesised as shown in Scheme 1. The sulfide **3**, prepared in high yield from commercially available starting materials, was reduced to the corresponding substituted aniline **4**. Succesive alkylations, in good yields, with propargyl bromide and 6-(bromomethyl)-3,4-dihydro-2-methyl-4-oxoquinazoline ("QCH_2Br")[4] rendered the key intermediate **6**. By careful selection of conditions, the sulfide **6** was oxidized to the sulfoxide **7** and separately to the sulfone **8**, each isolated by flash chromatography in a high state of purity. These new compounds were tested for their inhibition of human and *E. coli* TS and for their inhibition of the growth of three cell lines in tissue culture using methods previously described.[2] The results are shown in Table 1, which also contains our previous results for the sulfone **8d** and, as controls, the parent compounds **7a** and **8a**.[2]

Biological Results

The results for the inhibition of human and bacterial TS, listed in Table 1, show that the substituents X or Y generally induced minor changes in the K_i values, some of which were improvements. However, the two disubstituted compounds **7g** and **8g** were clearly less potent than their respective parent compounds. In the case of **8g** against the human enzyme, this loss was by 1 order of magnitude. Taking the sulfoxide series first, there is seen a slight selectivity for inhibition of the human enzyme across the whole series, parent compound **7a** included, and most observable for the methyl compound **7e**. The most potent sulfoxide inhibitor for both enzymes was the chloro compound **7c**, which, for the human enzyme, had a K_i of 27 nM. In the sulfone series, no compound improved upon the parent **8a** in inhibiting either enzyme, which was a disappointment. Compound **8f** with a distal chlorine substituent was the second best inhibitor of the human enzyme, having a K_i of 21 nM.

Turning to the tissue culture results, again structural variation induced little variation in the IC_{50} values. However, there were two exceptions to this generalization. First, disubstituted compounds **7g** and **8g** were

Table 1. Inhibition of Thymidylate Synthase and of Growth of Cells in Tissue Culture

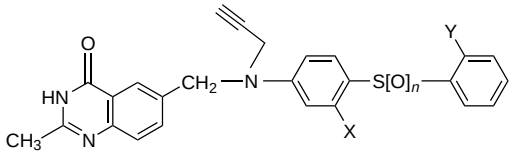

compd	X	Y	*n*	K_i[a] (μM) *E. coli* TS[d]	K_i[a] (μM) human TS[d]	IC_{50}[b] (μM) L1210	IC_{50}[b] (μM) CCRF-CEM	IC_{50}[b] (μM) GC_3/M TK^-	thymidine[c] shift
7a[e]	H	H	1	0.16 ± 0.08	0.061 ± 0.023				
				0.55 ± 0.04	0.11 ± 0.02	1.7	4.5	3.9	>5.3
7b	F	H	1	0.088 ± 0.042	0.050 ± 0.018				
				0.29 ± 0.16	0.12 ± 0.06	2.1	1.4	4.2	>2.3
7c	Cl	H	1	0.054 ± 0.018	0.027 ± 0.008				
				0.13 ± 0.03	0.037 ± 0.016	1.0	2.3	3.8	5.0
7d	CF_3	H	1	0.11 ± 0.06	0.070 ± 0.039				
				0.16 ± 0.09	0.15 ± 0.06	1.1	3.0	3.3	2.9
7e	H	CH_3	1	0.25 ± 0.11	0.045 ± 0.021				
				0.78 ± 0.28	0.077 ± 0.016	1.7	3.5	4.0	8.7
7f	H	Cl	1	0.19 ± 0.09	0.046 ± 0.019				
				0.76 ± 0.27	0.073 ± 0.025	2.1	5.8	4.3	3.8
7g	CF_3	CH_3	1	0.29 ± 0.1	0.26 ± 0.12				
				0.92 ± 0.41	0.39 ± 0.11	1.0	3.0	9.1	2.0
8a[e]	H	H	2	0.025 ± 0.006	0.012 ± 0.005				
				0.068 ± 0.05	0.021 ± 0.009	1.0	1.6	1.03	18.9
8b	F	H	2	0.043 ± 0.019	0.020 ± 0				
				0.074 ± 0.044	0.046 ± 0.013	1.2	2.0	2.8	>4.6
8c	Cl	H	2	0.033 ± 0.021	0.024 ± 0.012				
				0.043 ± 0.01	0.055 ± 0.018	1.6	1.5	3.0	4.6
8d[e]	CF_3	H	2	0.037 ± 0.019	0.050 ± 0.031				
				0.040 ± 0.008	0.084 ± 0.001	2.0	3.5	7.5	2.3
8e	H	CH_3	2	0.056 ± 0.025	0.026 ± 0.01				
				0.16 ± 0.06	0.058 ± 0.013	0.6	2.7	3.4	10.0
8f	H	Cl	2	0.033 ± 0.009	0.021 ± 0.007				
				0.069 ± 0.022	0.025 ± 0.012	0.3	0.6	1.2	6.1
8g	CF_3	CH_3	2	0.16 ± 0.08	0.15 ± 0.04				
				0.39 ± 0.21	0.38 ± 0.23	1.0	2.0	>5.0 (10%)	1.3

[a] For each compound the upper value is K_{is} and the lower K_{ii}. [b] For entries of the form >*x* (*y*%), *x* is the limiting solubility of the compound and *y* the percent inhibition at that concentration. [c] Expressed as the ratio of the IC_{50} for L1210 cells in the presence of 10 μM thymidine divided by the IC_{50} for the same cell line with no thymidine added. [d] Recombinant enzyme produced in *E. coli*. [e] Reference 2.

obviously less effective against the thymidine kinase-deficient human adenocarcinoma cell line GC_3/M TK^-, and second, the chloro sulfone **8f** was 3-fold more effective against each of the leukemic cell lines—murine L1210 and human CCRF-CEM. In each case these changes correlate qualitatively with changes in the inhibition of human TS as noted above. Considering both its inhibition of human TS and of the growth of cells, the chloro sulfone **8f** was clearly the best compound in the series. Thymidine reversal studies on the L1210 cell line were performed to investigate whether the compounds were acting upon TS when inhibiting growth. All compounds showed some degree of reversal. In the sulfoxide series the thymidine shift approximately tracked the human K_i potency (and less the IC_{50}), although the best compound was **7e** not **7c**. In the sulfone series, again the thymidine shift correlated more closely with K_i rather than IC_{50}; compound **8a** was clearly the most TS-directed. It is possible that the compounds act elsewhere in the folate enzyme network or even outside it; however, further mechanistic studies were not pursued.

Compound **8f**, noted above, was tested for *in vivo* antitumor activity. The compound was active in an antitumor model using mice inoculated with the thymidine kinase-deficient L5178Y (TK^-) murine lymphoma. A variety of doses and schedules of administration were tested. Optimal antitumor activity was found with a dose of 50 mg/kg given twice daily by intraperitoneal injection for 10 days. The group treated with compound **8f** displayed a mean increase in life span of more than 61% compared to the control-treated group. Unfortunately, *in vivo* testing of this compound was complicated by its poor aqueous solubility and its short half-life of approximately 30 min in mice.

Crystallography and Computational Chemistry

Two compounds only, **7e** and **7c** from the diphenyl sulfoxide series, cocrystallized with *E. coli* TS sufficiently well to be used for X-ray structural analysis. Figure 1 shows the 2.5 Å crystal structure of the TS complex with the methyl sulfoxide **7e**. Electron density for the sulfoxide oxygen is seen at a single location, indicating that *E. coli* TS binds one of the two enantiomers preferentially. A second feature of the binding of **7e** is that the distal methyl substituent has taken up the position pointing downward, not quite toward Ala262, but in the recognized alternative direction envisaged when it was modeled in the corresponding sulfone **8e**.

A clue to an explanation for this enantioselective binding of **7e** was obtained by considering the residues in the active site. These are shown in Figure 1 with a Connolly surface color coded for electrostatic potential calculated using the DELPHI program. The negative potential arising from Glu82, at the center-bottom of the view, extends upward and to the left, offering a possible destabilizing interaction to a sulfoxide oxygen

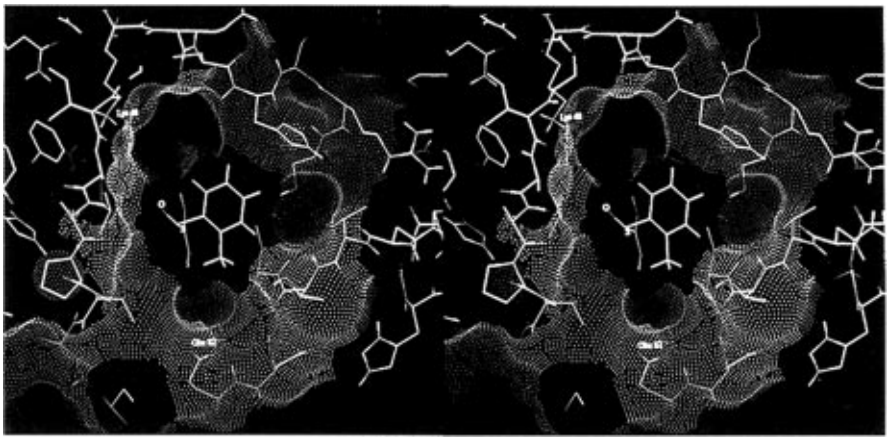

Figure 1. Stereopicture showing the experimentally determined structure of compound **7e** complexed to *E. coli* TS. The active site is outlined with a Connolly surface color coded to show electrostatic potential derived from DELPHI calculations. Surface of positive potential is colored red; neutral, green; and negative, blue. Both ligand and protein are shown in pale green for carbon, red for oxygen, blue for nitrogen, and yellow for sulfur. The oxygen of the sulfoxide is seen pointing toward the positive side chain nitrogen of Lys48 at top left. The negative side chain of Glu82 is at bottom right.

Table 2. Calculated Interaction Energies of Four Conformers of Compound **7e** with *E. coli* TS

		interaction energy of ligand with protein (kcal/mol)		
system[a]	conformation of molecule[b]	van der Waals	electrostatic	total
I	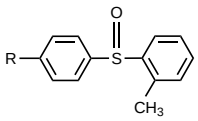	−64.8	−44.3	−109.1
II	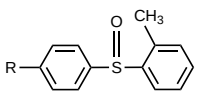	−66.1	−38.4	−104.5
III	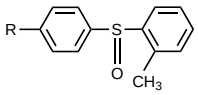	−62.8	−33.2	−96.0
IV	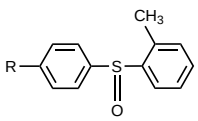	−65.4	−32.8	−98.2

[a] System I is shown in Figure 1. [b] Structure shows only the diphenyl sulfoxide moiety.

with a partial negative charge at that position. Conversely, Lys48, and the surrounding ordered solvent molecules, diametrically opposite in the site, offers a possible stabilizing interaction for the oxygen of the enantiomer that bound. This hypothesis was further explored by conformational analysis of **7e** in the active site of the enzyme. Molecular mechanics calculations (energy minimizations) on four different orientations of the ligand (Table 2) were performed using the AMBER force field[5,6] to determine the relative conformational preferences of the sulfoxide oxygen in the bound complex. The details of the systems setup, the calculation of force field parameters, and the partial atomic charges used are similar to those published in our earlier paper.[7] For the energy minimization of the protein inhibitor complex, a four-stage protocol was used. In the first stage, only the waters were minimized using 100 steps of steepest descent followed by 1000 steps of conjugate gradient methods, keeping the inhibitor and the protein fixed. The purpose of this step was to relieve any bad contacts in the initially solvated system. In the second stage, only hydrogens in the system were allowed to relax by 100 steps of steepest descent followed by 1000 steps of conjugate gradient. This step relaxes the hydrogen atoms prior to relaxing heavy atoms. It was performed because the hydrogen locations are not specified in the X-ray structure, and their adjustment is necessary to improve hydrogen bond geometries. In the third stage, only ligand and solvent water are moved (100 steps steepest descent plus 1000 steps conjugate gradient) by keeping the protein fixed. Finally, all the atoms of the residues within 25 Å from the center of the ligand are moved. This stage was performed using 100 steps of steepest descent and 5000 steps of conjugate gradient methods.

In the minimized structure for each complex, the interaction energy of the ligand with the protein atoms was calculated. This energy was decomposed into electrostatic and van der Waals contributions. These results are given in Table 2. The calculations show that the interaction energy of system I (−109.1 kcal/mol) is lower than that of its cis conformer, system II (−104.5 kcal/mol), but both are much lower than the energy of system III (−96.0 kcal/mol) or system IV (−98.2 kcal/mol), together representing the other enantiomer. The van der Waals contribution to the interaction energy varies by only 3.3 kcal/mol across the four systems; the systems are mostly differentiated by electrostatic energy. The 4.6 kcal/mol difference in interaction energy between conformers I and II of the bound enantiomer is not the only factor that favors binding of trans conformer I since cis isomer II has a higher internal energy (2.9 kcal by AMBER minimization).

The most reasonable interpretation of these results is that the most stable bound conformation (system I) is characterized by the polar sulfoxide oxygen engaging in a favorable electrostatic interaction with the positively charged residue Lys48. In contrast, oriented as in systems II and III, the sulfoxide oxygen loses this interaction and instead engages in an unfavorable electrostatic interaction with the negatively charged residue Glu82. This calculated lowest energy conformation (system I) for the ligand **7e** is in agreement with the observed experimental crystallographic result.

Enantiomeric selectivity by TS is apparently less stringent for the corresponding meta chlorosulfoxide

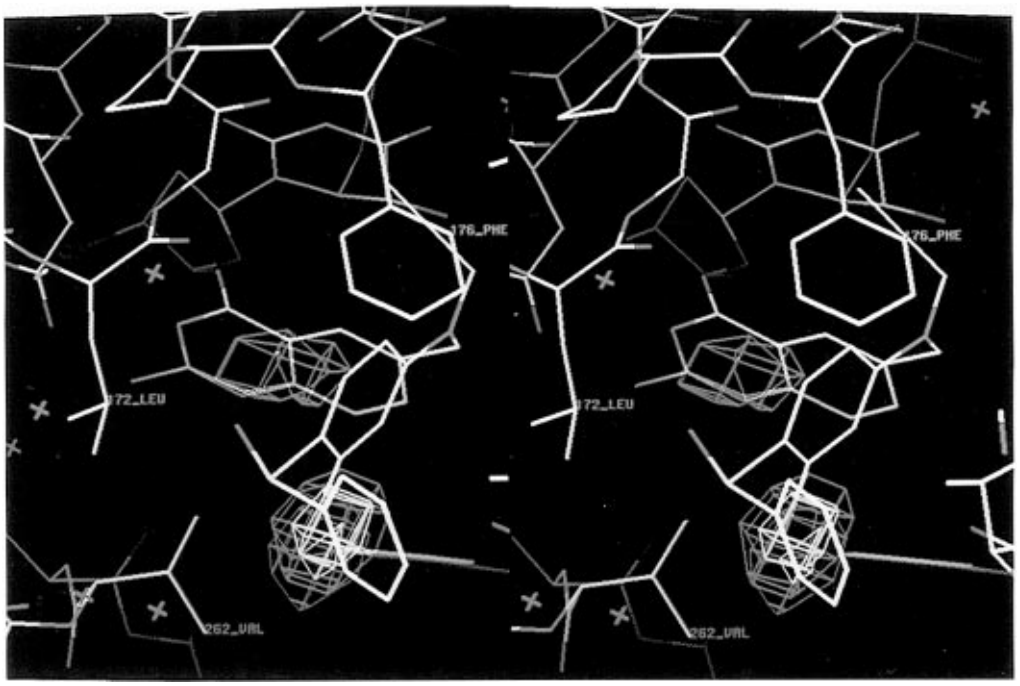

Figure 2. Stereopicture of difference electron density indicating two distinct positions for the chlorine of compound **7c** when complexed with *E. coli* TS and 5-FdUMP. The map is calculated at 2.5 Å resolution using coefficients $[F_{7c}-F_{8a}]$ where F_{7c} and F_{8a} are observed structure amplitudes for compounds **7c** and **8a**, respectively. Model phases were used with no contribution from the quinazoline inhibitor. The map is contoured at 8σ (red) and 12σ (yellow). The FdUMP molecule is visible below the quinazoline ring of compound **7c**.

analog **7c**. Chlorine substitution in **7c** is associated with strong difference density peaks appearing adjacent to both meta carbon atoms of the inhibitor's proximal phenyl ring (Figure 2). This indicates that either (i) a single enantiomer binds but the proximal phenyl of bound **7c** can flip about its long axis placing Cl cis or trans to the sulfoxide oxygen or (ii) both enantiomers bind (probably with their Cl and sulfoxide oxygens trans) but with different affinities. Since the X-ray experiment returns an electron density averaged over all populations in the crystal, we cannot eliminate the possibility that both enantiomers bind in both conformations. However, as for compound **7e** (*vide supra*), AMBER calculations indicate that the cis isomer has a significantly higher internal energy, suggesting that the two Cl peaks probably arise simply from binding both trans enantiomers. $2F_{7c}$-Fc difference maps (data not shown) reveal electron density for the sulfoxide oxygen in two positions consistent with the notion that both enantiomers of **7c** are bound in the cocrystal. Judging from the relative integrated peaks, the enantiomer with the sulfoxide oxygen pointed toward Lys48 predominates roughly 3 to 1. Further inspection of the difference density indicated a shift in the side chain of Phe176 as a result of 30−50° rotations around χ_1 and χ_2 in order to structurally accommodate the Cl of the more weakly bound enantiomer and such that the side chain had moved closer to the propargyl group of the inhibitor. No change in the enzyme structure around Phe176 was evident.

Discussion

We have described in this paper a series of new diphenyl sulfoxide and diphenyl sulfone inhibitors of the enzyme thymidylate synthase having a substituent in one or the other ring adjacent to the central sulfur and, in one case, with substituents in each ring. The enzyme inhibition measured for these compounds offered no or minor improvement over their unsubstituted parents. The probable reason for this outcome is that the pockets of the enzyme which the substituents were designed to occupy, particularly those for the distal substituents, were insufficiently defined and not deep enough to bury enough hydrophobic surface area to give the improvements in binding that were sought. The best compound, considering also tissue culture results, was the chloro sulfone **8f**. This compound was advanced to *in vivo* testing in lymphoma-bearing mice. It had definite activity since at a dose of 50 mg/kg it increased the life span of the mice by more than 61%. However, its poor aqueous solubility combined with its disadvantageous short half-life in mice of only 30 min deterred us from investigating it further.

Two interesting results were obtained from the crystallographic analysis. In the first there was observed a selective binding to *E. coli* TS of one enantiomer of the sulfoxide, **7e**. The likely explanation for this phenomenon is that the positively-charged Lys48 and the negatively-charged Glu82 at the mouth of the active site act in concert to favor the binding of one enantiomer by electrostatic effects. Molecular mechanics calculations performed with the AMBER force field validated this explanation. It cannot be extrapolated that such enantioselective binding occurs with human TS because, although Lys48 is conserved, the residue corresponding to Glu82 is Ala in that enzyme. The second crystal structure revealed that the side chain of Phe 176 had rotated sideways and back into the enzyme to make room for the meta chlorine substituent of the sulfoxide **7c** to take partial occupancy by hydrophobic interaction. In three previous crystal structures we presented with the meta substituents CF_3[1] and CH_2OH,[2] this phenomenon was not observed. Unlike **7e**, both enantiomers of **7c** appeared to bind to TS. The clear result was that

Phe176 was a residue with a hitherto unrecognized flexibility of movement and that the *E. coli* enzyme, and by extension the human enzyme, was capable of accepting trisubstituted compounds with substituents at positions 3, 4, *and* 5 relative to the N^{10} aniline nitrogen. Thus the crystal structure of compound **7c** bound to TS immediately suggested the next iteration of design and synthesis, and this will be described in a future paper.

Experimental Section

Protocols for chemistry, crystallography, and *in vitro* biology were previously described.[2] Every intermediate (**3**−**6**) described below had a satisfactory ^{1}H NMR spectrum in the solvent stated; chemical shifts and couplings typical of each compound class have been detailed.[2]

General Method for Preparation of the Sulfides 3. A solution of the thiol **2** (10 mmol) in THF (about 90 mL) in a flame-dried flask under argon was treated with NaH (10 mmol) at 0−3 °C with ice cooling. Following the addition, the salt solution was allowed to warm to room temperature during 30−45 min and then treated with the fluoride **1** (10 mmol). Reaction usually took place at room temperature but was completed at 60 °C. Extractive workup (hexane/H_2O) gave the product **3**.

3-Fluoro-4-(phenylthio)nitrobenzene (3b): yellow prisms (95%); mp 53.5−54.5 °C (EtOH); NMR (Me_2SO-d_6). Anal. ($C_{12}H_8FNO_2S$) C, H, N, S.

3-Chloro-4-(phenylthio)nitrobenzene (3c): large yellow crystals (73%); mp 117−118.5 °C (EtOH); NMR (Me_2SO-d_6). Anal. ($C_{12}H_8ClNO_2S$) C, H, N, Cl, S (lit.[8]).

4-(Phenylthio)-3-(trifluoromethyl)nitrobenzene (3d): oil (90%); NMR ($CDCl_3$). Anal. ($C_{13}H_8F_3NO_2S$) C, H, N, F, S (lit.[9]).

4-((2-Methylphenyl)thio)nitrobenzene (3e): solid (96%); mp 42−46 °C (hexanes); NMR ($CDCl_3$). Anal. ($C_{13}H_{11}NO_2S$) C, H, N, S (lit.[10] 64−65 °C).

4-((2-Chlorophenyl)thio)nitrobenzene (3f): solid (92%); mp 105−107 °C (hexanes); NMR ($CDCl_3$). Anal. ($C_{12}H_8ClNO_2S \cdot 0.1C_6H_{14}$) C, H, N, Cl, S (lit.[10] 113−114 °C).

4-((2-Methylphenyl)thio)-3-(trifluoromethyl)nitrobenzene (3g): solid (83%); mp 42−45 °C (hexane); NMR ($CDCl_3$). Anal. ($C_{14}H_{10}F_3NO_2S$) C, H, N, S.

General Method for Preparation of the Anilines 4. The nitrobenzene **3** (*q* mmol) was dissolved in a warm (50−60 °C) solution of $SnCl_2 \cdot 2H_2O$ (5*q* mmol) in EtOH (1−1.5*q* mL) in a beaker. Concentrated HCl (1−1.5*q* mL) was added and the mixture heated at 60 °C for 15−30 min to remove most of the EtOH. The cooled mixture was basified to pH >> 12 with $NaOH_{aq}$ and the product isolated by filtration and/or extraction.

3-Fluoro-4-(phenylthio)aniline (4b): white needles (92%); mp 87−88.5 °C (EtOH); NMR ($CDCl_3$). Anal. ($C_{12}H_{10}FNS$) C, H, N, F, S.

3-Chloro-4-(phenylthio)aniline (4c): white solid (96%); mp 48−49 °C; NMR (Me_2SO-d_6). Anal. ($C_{12}H_{10}ClNS$) C, H, N, Cl, S (lit.[11]).

4-(Phenylthio)-3-(trifluoromethyl)aniline (4d): yellow oil (100%); NMR ($CDCl_3$). Anal. ($C_{13}H_{10}F_3NS$) C, H, N, F, S (lit.[12]).

4-((2-Methylphenyl)thio)aniline (4e): solid (44%); mp 50−51 °C (hexanes); NMR ($CDCl_3$). Anal. ($C_{13}H_{13}NS$) C, H, N, S (lit.[13] mp 50 °C).

4-((2-Chlorophenyl)thio)aniline (4f): solid (71%); mp 72−74 °C (hexanes); NMR ($CDCl_3$). Anal. ($C_{12}H_{10}ClNS \cdot 0.2C_6H_{14}$) C, H, N, Cl, S (lit.[10] mp 77−78 °C).

4-((2-Methylphenyl)thio)-3-(trifluoromethyl)aniline (4g): oil (96%); NMR ($CDCl_3$). Anal. ($C_{14}H_{12}F_3NS$) C, H, N, S.

Propargylanilines 5. Reactions were conducted and the products purified by methods previously described.[2]

3-Fluoro-4-(phenylthio)-*N*-(prop-2-ynyl)aniline (5b): oil (42%); NMR (Me_2SO-d_6). Anal. ($C_{15}H_{12}FNS \cdot 0.25H_2O$) C, H, N, S.

3-Chloro-4-(phenylthio)-*N*-(prop-2-ynyl)aniline (5c): oil (36%); NMR (Me_2SO-d_6). Anal. ($C_{15}H_{12}ClNS$) C, H, N, Cl, S.

4-(Phenylthio)-*N*-(prop-2-ynyl)-3-(trifluoromethyl)aniline (5d): yellow oil (53%); NMR (Me_2SO-d_6). Anal. ($C_{16}H_{12}F_3NS$) C, H, N, F, S.

4-((2-Methylphenyl)thio)-*N*-(prop-2-ynyl)aniline (5e): oil (68%); NMR ($CDCl_3$). Anal. ($C_{16}H_{15}NS$) C, H, N, S.

4-((2-Chlorophenyl)thio)-*N*-(prop-2-ynyl)aniline (5f): oil (69%); NMR ($CDCl_3$). Anal. ($C_{15}H_{12}ClNS$) C, H, N, Cl, S.

4-((2-Methylphenyl)thio)-*N*-(prop-2-ynyl)-3-(trifluoromethyl)aniline (5g): oil (51%); NMR ($CDCl_3$). Anal. ($C_{17}H_{14}F_3NS \cdot 0.25H_2O$) C, H, N, S.

Quinazoline Sulfides 6. Reactions were conducted and the products purified by methods previously described.[2]

***N*-((3,4-Dihydro-2-methyl-4-oxo-6-quinazolinyl)methyl)-3-fluoro-4-(phenylthio)-*N*-(prop-2-ynyl)aniline (6b):** white solid (51%); mp 221−223 °C dec (CH_3CN/CCl_4); NMR (Me_2SO-d_6). Anal. ($C_{25}H_{20}FN_3OS$) C, H, N, F, S.

3-Chloro-*N*-((3,4-dihydro-2-methyl-4-oxo-6-quinazolinyl)methyl)-4-(phenylthio)-*N*-(prop-2-ynyl)aniline (6c): white solid (20%); mp 224 °C dec (CH_3CN/CCl_4); NMR (Me_2SO-d_6). Anal. ($C_{25}H_{20}ClN_3OS$) C, H, N, Cl, S.

***N*-((3,4-Dihydro-2-methyl-4-oxo-6-quinazolinyl)methyl)-4-(phenylthio)-*N*-(prop-2-ynyl)-3-(trifluoromethyl)aniline (6d):** off-white solid (23%); mp 228−230 °C; NMR ($CDCl_3$). Anal. ($C_{26}H_{20}F_3N_3OS \cdot H_2O$) C, H, N.

***N*-((3,4-Dihydro-2-methyl-4-oxo-6-quinazolinyl)methyl)-4-((2-methylphenyl)thio)-*N*-(prop-2-ynyl)aniline (6e):** off-white solid (90%); mp 192−194 °C ($CHCl_3$/MeOH); NMR ($CDCl_3$). Anal. ($C_{26}H_{23}N_3OS \cdot H_2O$) C, H, N.

4-((2-Chlorophenyl)thio)-*N*-((3,4-dihydro-2-methyl-4-oxo-6-quinazolinyl)methyl)-*N*-(prop-2-ynyl)aniline (6f): pale yellow solid (26%); mp 215−217 °C dec ($CHCl_3$); NMR (Me_2SO-d_6). Anal. ($C_{25}H_{20}ClN_3OS \cdot 0.6H_2O$) C, H, N, Cl, S.

***N*-((3,4-Dihydro-2-methyl-4-oxo-6-quinazolinyl)methyl)-4-((2-methylphenyl)thio)-*N*-(prop-2-ynyl)-3-(trifluoromethyl)aniline (6g):** off-white solid (45%); mp 219−222 °C ($CHCl_3$/MeOH); NMR (Me_2SO-d_6). Anal. ($C_{27}H_{22}F_3N_3OS$) C, H, N, S.

Preparation of Sulfoxides 7: Method A. The sulfide **6b** or **6c** (*y* mmol) was dissolved in HOAc (100*y* mL) and treated with $NaBO_3 \cdot 4H_2O$ (*y* mmol). The mixture was stirred (**6b**/2 h/45 °C; **6c**/23 h/60 °C) and then poured into saturated aqueous $NaHCO_3$. Extractive (CH_2Cl_2) workup followed by flash chromatography on silica using the eluant stated gave the pure product. **Method B.** The sulfides **6d**,**e**,**f**,**g** (*y* mmol) were dissolved in HOAc (20*y* mL) and treated with H_2O_2 (30%, 1.5*y* mmol, 1.5 equiv). The mixture was stirred 16 h at 25 °C and then poured into saturated aqueous $NaHCO_3$. Extractive ($CHCl_3$) workup followed by flash chromatography on silica using the eluant stated gave the pure product.

***N*-((3,4-Dihydro-2-methyl-4-oxo-6-quinazolinyl)methyl)-3-fluoro-4-(phenylsulfinyl)-*N*-(prop-2-ynyl)aniline (7b):** eluant, toluene 50%−CH_3CN 48%−MeOH 2%; white solid (13%); mp 228.5−229.5 °C dec; NMR (Me_2SO-d_6) δ 2.32 (s, 3H), 3.25 (t, 1H), 4.34 (d, 2H), 4.77 (s, 2H), 6.67 (dd, 1H), 6.76 (dd, 1H), 7.38−7.67 (m, 8H), 7.93 (d, 1H), 12.20 (s, 1H). Anal. ($C_{25}H_{20}FN_3O_2S$) C, H, N, F, S.

3-Chloro-*N*-((3,4-dihydro-2-methyl-4-oxo-6-quinazolinyl)methyl)-4-(phenylsulfinyl)-*N*-(prop-2-ynyl)aniline (7c): eluant, toluene 50%−CH_3CN 48%−MeOH 2%; white solid (33%); mp 233−234 °C dec; NMR (Me_2SO-d_6) δ 2.32 (s, 3H), 3.27 (t, 1H), 4.35 (d, 2H), 4.77 (s, 2H), 6.87 (d, 1H), 6.95 (dd, 1H), 7.50−7.67 (m, 8H), 7.94 (d, 1H), 12.20 (s, 1H). Anal. ($C_{25}H_{20}ClN_3O_2S$) C, H, N, Cl, S.

***N*-((3,4-Dihydro-2-methyl-4-oxo-6-quinazolinyl)methyl)-4-(phenylsulfinyl)-*N*-(prop-2-ynyl)-3-(trifluoromethyl)aniline (7d):** eluant, EtOAc; white solid (90%); mp 226−228 °C dec; NMR ($CDCl_3$) δ 2.30 (t, lH, J = 2.1 Hz), 2.54 (s, 3H), 4.15 (d, 2H, J = 2.1 Hz), 4.74 (s, 2H), 7.04−7.07 (m, 2H), 7.40−7.46 (m, 3H), 7.61−7.65 (m, 4H), 7.88 (d, lH, J = 8.5 Hz), 8.13 (s, lH), 11.17 (br s, lH). Anal. ($C_{26}H_{20}F_3N_3O_2S \cdot 0.5H_2O$) C, H, N, S.

***N*-((3,4-Dihydro-2-methyl-4-oxo-6-quinazolinyl)methyl)-4-((2-methylphenyl)sulfinyl)-*N*-(prop-2-ynyl)aniline (7e):** eluant, EtOAc; off-white solid (72%); mp 197−198 °C dec (EtOAc); NMR ($CDCl_3$) δ 2.23 (s, 3H), 2.26 (t, 1H, J = 2.3 Hz), 2.55 (s, 3H), 4.11 (d, 2H, J = 2.3 Hz), 4.70 (s, 2H), 6.85 (d, 2H,

J = 9.0 Hz), 7.14 (d, 1H, J = 7.4 Hz), 7.35 (dt, 1H, J= 7.4, 1.4 Hz), 7.45 (m, 3H), 7.64 (s, 2H), 8.07 (dd, 1H, J = 7.7, 1.3 Hz), 8.14 (s, 1H), 11.40 (br s, 1H). Anal. ($C_{26}H_{23}N_3O_2S\cdot0.2H_2O$) C, H, N, S.

4-((2-Chlorophenyl)sulfinyl)-*N*-((3,4-dihydro-2-methyl-4-oxo-6-quinazolinyl)methyl)-*N*-(prop-2-ynyl)aniline (7f): eluant, CH_2Cl_2 95%−MeOH 5%; pale yellow solid (48%); mp 221−223 °C dec (CH_2Cl_2/MeOH); NMR ($CDCl_3$) δ 2.27 (t, 1H, J = 2.2 Hz), 2.55 (s, 3H), 4.11 (d, 2H, J = 2.1 Hz), 4.70 (s, 2H), 6.85 (d, 2H, J = 9.0 Hz), 7.32 (dt, 1H, J = 8.4, 1.5 Hz), 7.37 (dt, 1H, J = 7.2, 1.5 Hz), 7.53 (m, 3H), 7.64 (s, 2H), 8.12 (m, 2H), 11.30 (br s, 1H). Anal. ($C_{25}H_{20}ClN_3O_2S$) C, H, N, Cl, S.

***N*-((3,4-Dihydro-2-methyl-4-oxo-6-quinazolinyl)methyl)-4-((2-methylphenyl)sulfinyl)-*N*-(prop-2-ynyl)-3-(trifluoromethyl)aniline (7g):** eluant, CH_2Cl_2 95%−MeOH 5%; off-white solid (45%); mp 216−218 °C dec ($CHCl_3$/MeOH); NMR (Me_2SO-d_6) δ 2.12 (s, 3H), 2.32 (s, 3H), 3.32 (t, 1H, J = 2.2 Hz), 4.46 (d, 2H, J = 1.9 Hz), 4.85 (s, 2H), 7.16 (m, 2H), 7.31 (m, 2H), 7.50 (m, 3H), 7.65 (d, 1H, J = 7.3 Hz), 7.77 (d, 1H, J = 7.3 Hz), 7.96 (d, 1H, J = 1.8 Hz), 12.20 (br, s, 1H). Anal. ($C_{27}H_{22}F_3N_3O_2S$) C, H, N, F, S.

Preparation of Sulfones 8: Method A. The sulfide **6c** or **6e** (y mmol) was dissolved in $CHCl_3$ (200y mL) and treated with MCPBA (50−60%, 2y mmol, 2 equiv). The mixture was stirred for approximately 17 h at 25 °C and then poured into saturated aqueous $NaHCO_3$. Extractive ($CHCl_3$) workup followed by flash chromatography on silica using the eluant stated gave the pure product. **Method B.** The sulfides **6b**,**f**,**g** (y mmol) were dissolved in HOAc (100y mL) and treated with H_2O_2 (30%, 5y mmol, 5 equiv). The mixture was stirred 23 h at 40−60 °C and then poured into saturated aqueous $NaHCO_3$. Extractive (CH_2Cl_2) workup followed by flash chromatography on silica using the eluant stated gave the pure product.

***N*-((3,4-Dihydro-2-methyl-4-oxo-6-quinazolinyl)methyl)-3-fluoro-4-(phenylsulfonyl)-*N*-(prop-2-ynyl)aniline (8b):** eluant, toluene 60%−CH_3CN 38%−MeOH 2%; cream-colored solid (5%); mp 237.5−239 °C dec (CH_3CN/CCl_4); NMR (Me_2SO-d_6) δ 2.32 (s, 3H), 3.29 (t, 1H), 4.38 (d, 2H), 4.82 (s, 2H), 6.68 (dd, 1H), 6.76 (dd, 1H), 7.52 (m, 9H), 12.21 (s, 1H). Anal. ($C_{25}H_{20}FN_3O_3S$) C, H, N, F, S.

3-Chloro-*N*-((3,4-dihydro-2-methyl-4-oxo-6-quinazolinyl)methyl)-4-(phenylsulfonyl)-*N*-(prop-2-ynyl)aniline (8c): eluant for first chromatography, CCl_4 55%−CH_3CN 35%−Et_2O 10%; eluant for second chromatography, toluene 50%−CH_3CN 48%−MeOH 2%; pale yellow solid (43%); mp 242−243.5 °C dec (CH_3CN/CCl_4); NMR (Me_2SO-d_6) δ 2.32 (s, 3H), 3.30 (t, 1H), 4.42 (d, 2H), 4.80 (s, 2H), 6.90 (d, 1H), 6.94 (dd, 1H), 7.53−7.69 (m, 5H), 7.84 (m, 2H), 7.94 (d, 1H), 8.02 (d, 1H), 12.21 (s, 1H). Anal. ($C_{25}H_{20}ClN_3O_3S$) C, H, N, Cl, S.

***N*-((3,4-Dihydro-2-methyl-4-oxo-6-quinazolinyl)methyl)-4-((2-methylphenyl)sulfonyl)-*N*-(prop-2-ynyl)aniline (8e):** eluant, EtOAc; cream-colored solid (65%); mp 186−188 °C dec (EtOAc); NMR ($CDCl_3$) δ 2.29 (t, 1H, J = 2.4 Hz), 2.49 (s, 3H), 2.56 (s, 3H), 4.16 (d, 2H, J = 2.2 Hz), 4.75 (s, 2H), 6.86 (d, 2H, J = 8.8 Hz), 7.20 (d, 1H, J = 7.4 Hz), 7.33 (t, 1H, J = 7.5 Hz), 7.47 (dt, 1H, J = 7.4, 1.4 Hz), 7.65 (d, 2H, J = 1.5 Hz), 7.72 (d, 2H, J = 9.2 Hz), 8.14 (m, 2H), 11.35 (br s, 1H). Anal. ($C_{26}H_{23}N_3O_3S\cdot0.6H_2O$) C, H, N, S.

4-((2-Chlorophenyl)sulfonyl)-*N*-((3,4-dihydro-2-methyl-4-oxo-6-quinazolinyl)methyl)-*N*-(prop-2-ynyl)aniline (8f): eluant, EtOAc; pale yellow solid (44%); mp 219−220 °C dec (EtOAc); NMR ($CDCl_3$) δ 2.30 (t, 1H, J = 2.2 Hz), 2.54 (s, 3H), 4.17 (d, 2H, J = 2.2 Hz), 4.76 (s, 2H), 6.84 (d, 2H, J = 9.1 Hz), 7.42 (m, 3H), 7.64 (d, 2H, J = 1.3 Hz), 7.80 (d, 2H, J = 9.1 Hz), 8.11 (s, 1H), 8.26 (d, 1H, J = 7.0 Hz), 10.95 (br s, 1H). Anal. ($C_{25}H_{20}ClN_3O_3S$) C, H, N, Cl, S.

***N*-((3,4-Dihydro-2-methyl-4-oxo-6-quinazolinyl)methyl)-4-((2-methylphenyl)sulfonyl)-*N*-(prop-2-ynyl)-3-(trifluoromethyl)aniline (8g):** eluant, $CHCl_3$ 97%−MeOH 3%; off-white solid (43%); mp 169−171 °C dec ($CHCl_3$/MeOH); NMR (Me_2SO-d_6) δ 2.33 (s, 3H), 2.40 (s, 3H), 3.35 (t, 1H, J = 2.2 Hz), 4.53 (d, 2H, J = 2.2 Hz), 4.93 (s, 2H), 7.20 (m, 2H), 7.36 (m, 2H), 7.57 (m, 2H), 7.69 (dd, 1H, J = 8.5, 2.1 Hz), 7.77 (d, 1H, J = 7.8 Hz), 7.98 (d, 1H, J = 2.2 Hz), 8.03 (d, 1H, J = 9.0 Hz), 12.25 (br s, 1H). Anal. ($C_{27}H_{22}F_3N_3O_3S$) C, H, N, F.

Measurement of *in Vivo* Antitumor Activity. L5178Y (TK^-), a thymidine kinase-deficient murine lymphoma, was inoculated by intraperitoneal injection (ip) into $B6D2F_1$ mice at a concentration of 1×10^6 cells/mouse. Treatment began on the following day with either compound **8f** or vehicle delivered by ip injection. Compound **8f** was dissolved in *N*,*N*-dimethylacetamide (DMA), and this solution was diluted with a solution of (hydroxypropyl)-β-cyclodextrin (Molecusol, 45% w/v) to give the injectable solution with a concentration of 5 mg/mL of **8f** and 1.7% DMA.

Control-treated animals received vehicle. There were six animals in each group. The day of death was recorded for each animal and used to calculate the mean day of death for each group. The increase in life span (ILS) for the **8f**-treated group was calculated as follows:

$$\text{ILS (\%)} = \text{mean day of death } \frac{[\textbf{8f} \text{ group} - \text{control group}]}{[\text{control group}]} \times 100$$

References

(1) Appelt, K.; Bacquet, R. J.; Bartlett, C. A.; Booth, C. L. J.; Freer, S. T.; Fuhry M. A. M.; Gehring, M. R.; Herrmann, S. M.; Howland, E. F.; Janson, C. A.; Jones, T. R.; Kan, C.-C.; Kathardekar, V.; Lewis, K. K.; Marzoni, G. P.; Matthews, D. A.; Mohr, C.; Moomaw, E. W.; Morse, C. A.; Oatley, S. J.; Ogden, R. C.; Reddy, M. R.; Reich, S. H.; Schoettlin, W. S.; Smith, W. W.; Varney, M. D.; Villafranca, J. E.; Ward, R. W.; Webber, S.; Webber, S. E.; Welsh, K. M.; White, J. Design of enzyme inhibitors using iterative protein crystallographic analysis. *J. Med. Chem.* **1991**, *34*, 1925−1934.

(2) Jones, T. R.; Varney, M. D.; Webber, S. E.; Lewis, K. K.; Marzoni, G. P.; Palmer, C. L.; Kathardekar, V.; Welsh, K. M.; Webber, S.; Matthews, D. A.; Appelt, K.; Smith, W. W.; Janson, C. A.; Villafranca, J. E.; Bacquet, R. J.; Howland, E. F.; Booth, C. L. J.; Herrmann, S. M.; Ward, R. W.; White, J.; Moomaw, E. W.; Bartlett, C. A.; Morse, C. A. Structure-based design of lipophilic quinazoline inhibitors of thymidylate synthase. *J. Med. Chem.* **1996**, *39*, 904−917.

(3) Matthews, D. A.; Appelt, K.; Oatley, S. J.; Xuong, Ng. H. Crystal structure of *Escherichia coli* thymidylate synthase containing bound 5-fluoro-2′-deoxyuridylate and 10-propargyl-5,8-dideazafolate. *J. Mol. Biol.* **1990**, *214*, 923−936.

(4) Hughes L. R.; Jackman, A. L.; Oldfield, J.; Smith, R. C.; Burrows, K. D.; Marsham, P. R.; Bishop, J. A. M.; Jones, T. R.; O'Connor, B. M.; Calvert, A. H. Quinazoline antifolate thymidylate synthase inhibitors: Alkyl, substituted alkyl, and aryl substituents in the C2 position. *J. Med. Chem.* **1990**, *33*, 3060−3067.

(5) Weiner, S. J.; Kollman, P. A.; Case, D. A.; Singh, U. C.; Ghio, C.; Alagona, G.; Profeta, S., Jr.; Weiner, P. A new force field for moecular mechanical simulation of nucleic acids and proteins. *J. Am. Chem. Soc.* **1984**, *106*, 765−784.

(6) Singh, U. C.; Weiner, P. K.; Caldwell, J. K.; Kollman, P. A. *AMBER* (*Version 3.3*); University of California: San Francisco, 1986.

(7) Reddy, M. R.; Bacquet, R. J.; Zichi, D.; Matthews, D. A.; Welsh, K. M.; Jones, T. R.; Freer, S. Calculation of solvation and binding free energy differences for folate-based inhibitors of the enzyme thymidylate synthase. *J. Am. Chem. Soc.* **1992**, *114*, 10117−10122.

(8) Hamada, Y.; Matsuoka, H.; Hayashi, M. *Yakugashi Zasshi* **1970**, *90*, 644−646.

(9) Stacy, G. W.; Bresson, C. R.; Harmon, R. E.; Thamm, R. C. Preparation of some aminotrifluoromethyldiphenyl sulfones as possible antibacterial agents. *J. Org. Chem.* **1957**, *22*, 298−302.

(10) Gilman, H.; Broadbent, H. S. Some basically substituted diaryl sulfides and sulfones. *J. Am. Chem. Soc.* **1947**, *69*, 2053−2057.

(11) Singhal, G. P. U.S. Patent 3,576,872, April 27, 1971.

(12) Loeffler, R. S. T.; Woodcock, D.; Carter, G. A.; Johnson, D. M. Structure-activity relationships in fungitoxicants related to triforine and chloraniformethan. Part IV. Evaluation of the predictive power of the Hansch analysis by the preparation and testing of further chloraniformethan analogs. *Pestic. Sci.* **1981**, *12*, 627−637.

(13) Heiduschka, A.; Langkammerer, H. Über p- und o-toluolsulfinsäure. *J. Prakt. Chem., Ser. 2.* **1913**, *88*, 425−442.

JM960613F